Atomic Mapping of the Interactions between the Antiviral Agent Cyanovirin-N and Oligomannosides by Saturation-Transfer Difference NMR†

Corine Sandström,*,‡ Olivier Berteau,‡ Emiliano Gemma,§ Stefan Oscarson,§ Lennart Kenne,‡ and Angela M. Gronenborn||

Department of Chemistry, Swedish University of Agricultural Sciences, Post Office Box 7015, SE-750 07 Uppsala, Sweden, Department of Organic Chemistry, Arrhenius Laboratory, Stockholm University, SE-106 91 Stockholm, Sweden, and Laboratory of Chemical Physics, National Institute of Diabetes and Digestives and Kidney Diseases, National Institutes of Health, Bethesda, Maryland 20892

Received June 24, 2004; Revised Manuscript Received August 27, 2004

ABSTRACT: The minimum oligosaccharide structure required for binding to the potent HIV-inactivating protein cyanovirin-N (CV-N) was determined by saturation-transfer difference (STD) NMR spectroscopy. Despite the low molecular mass of the protein (11 kDa), STD-NMR spectroscopy allowed the precise atomic mapping of the interactions between CV-N and various di- and trimannosides, substructures of Man-9, the predominant oligosaccharide on the HIV viral surface glycoprotein gp120. Contacts with mannosides containing the terminal Manα(1→2)Manα unit of Man-9 were observed, while (1→3)- and (1−6)-linked di- and trimannosides showed no interactions, demonstrating that the terminal Manα(1→2)-Manα structure plays a key role in the interaction. Precise epitope mapping revealed that, for Manα-(1→2)Manα*O*Me, Manα(1→2)Manα(1→3)Manα*O*Me, and Manα(1→2)Manα(1→6)Manα*O*Me, the protein is in close contact with H2, H3, and H4 of the nonreducing terminal mannose unit. In contrast, the STD-NMR spectrum of the CV-N/trisaccharide Manα(1→2)Manα(1→2)Manα*O*Me complex was markedly different, with resonances on all sugar units displaying equal enhancements, suggesting that CV-N is able to discriminate between the three structurally related trisaccharides.

Cyanovirin-N (CV-N) is an 11-kDa protein, isolated from aqueous extracts of the cyanobacterium *Nostoc ellipsosporum* (*1*), that has attracted widespread interest because of its ability to neutralize diverse strains of HIV. CV-N not only prevents virus−cell fusion but also cell−cell fusion resulting in efficient inhibition of infection. Furthermore, the therapeutic spectrum of CV-N is broad, including other enveloped viruses, such as feline immunodeficiency virus, herpes virus 6, measles virus (*2*), and Ebola virus (*3*). It is therefore of critical importance to detail the inhibitory mechanism of CV-N to further its development as a topical antiviral agent and to gain insight into the involvement of carbohydrates in infectious diseases. In the case of HIV, it has been shown that the antiviral properties of CV-N are mediated by binding to highly glycosylated viral surface envelope proteins such as gp120, and particularly to the N-linked high mannose oligosaccharides, Man-8 and Man-9 (*1*, *4*−*7*).

To date, several crystal and NMR structures have been solved (*8*−*11*) and two carbohydrate-binding sites have been identified on the surface of CV-N, exhibiting slightly different affinities for di- and trisaccharides (7, *12*, *15*). Site 1 on domain B (residues 39−89) consists of a deep pocket, while site 2 on domain A (residues 1−38/90−101) is a shallow semicircular cleft (*13*). Sugar titrations and chemical-shift-mapping studies performed on a series of synthetic oligomannosides, substructures of Man-9 (Figure 1), indicated that the minimum structure required for binding comprises the disaccharide Manα(1→2)Manα (*13*−*17*). The bound sugars were found with the nonreducing mannopyranose ring stacked over the reducing mannopyranose ring *(11, 13*). NMR and isothermal titration calorimetry data revealed that the trisaccharides Manα(1→2)Manα(1→2)-Manα, Manα(1→2)Manα(1→3)Manα, and Manα(1→2)-Manα(1→6)Manα bound to the protein on domains A and B in the micromolar range *(14, 15)* as did the disaccharide Manα(1→2)Manα (*12*).

In this work, we have used saturation transfer difference (STD) NMR (*18*−*20*) to detect direct contacts between the protein and the sugar to further investigate and determine the specificity with respect to various di- and trimannosides (Figure 1), all substructures of Man-9. In STD-NMR, magnetization is transferred from the protein to the ligand, thereby identifying the binding of the ligand, and, more importantly, delineating the precise binding epitope on the ligand.

EXPERIMENTAL PROCEDURES

Each NMR sample contained 78 μM cyanovirin-N and a 42-fold (or 100-fold) excess of one of the oligosaccharides

† This work was supported by the European Network Glycotrain (HPRN-CT2000-00001), the Swedish Research Council, and the Intramural AIDS Targeted Antiviral Program of the Office of the Director of the National Institutes of Health (to A.M.G.).

* To whom correspondence should be addressed. E-mail: corine.sandstrom@kemi.slu.se. Telephone: +46 (0)18 67 15 68. Fax: +46 (0)18 67 34 76.

‡ Swedish University of Agricultural Sciences.

§ Stockholm University.

|| National Institutes of Health.

10.1021/bi048676k CCC: $27.50
Published on Web 10/13/2004

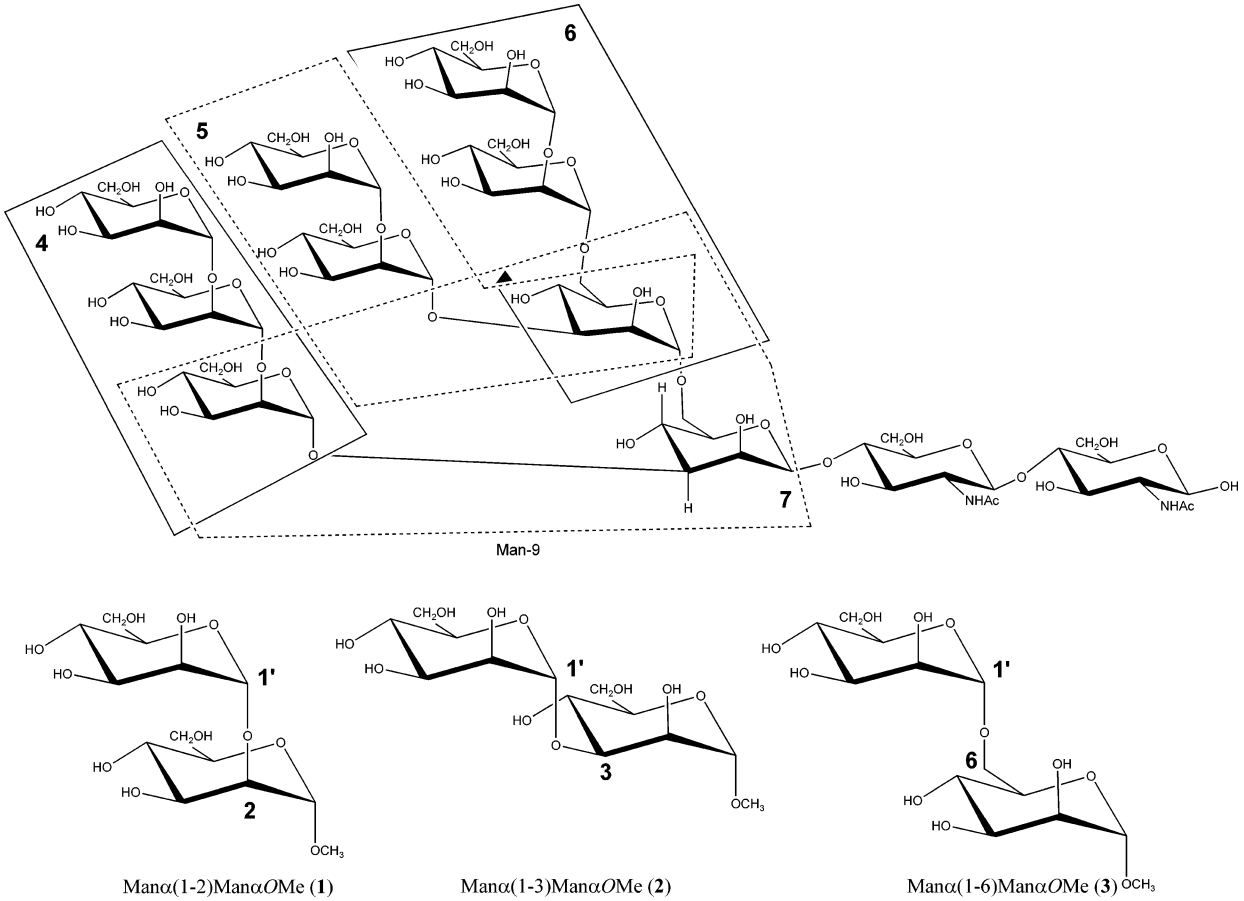

FIGURE 1: Chemical structures of $Man_9GlcNAc_2$ and disaccharides **1**−**3**.

1−**7**, in 20 mM sodium phosphate buffer at pH 6.0, 0.05% NaN_3, and 99.96% D_2O. All NMR spectra were recorded on a Bruker DRX 600 spectrometer using a 5-mm inverse-detection probe equipped with a z gradient. Spectra were acquired at 10 and 25 °C with the HDO signal as the internal reference (4.94 ppm at 10 °C and 4.75 ppm at 25 °C), and it was established that the STD-NMR intensities were stronger at 10 °C (see the Supporting Information). The predominant factor for STD enhancement at low temperature has been attributed to the reduced molecular tumbling of the molecular complex (*21*). 1D STD-NMR experiments were recorded with 2048 or 4096 scans, and water suppression was achieved using the WATERGATE pulse sequence (*22*). Saturation of the protein magnetization was carried out using a pulse train of 40 Gaussians of 50-ms duration, each separated by a 1-ms delay. Spectra were acquired with on-resonance frequencies set at 0.25, 0.4, 0.6, 1.3, 2, and 7 ppm, and the reference STD spectra were recorded with the off-resonance set at 30 ppm. Saturation times of 0.5 and 1−6 s incremented in 1-s steps were used. Saturated spectra were subtracted from the reference spectra via phase cycling.

Because the size of CV-N (11 kDa) is very close to the limit of 10 kDa, suggested to be the smallest size for which effective saturation of the entire protein by spin diffusion can be achieved and thus rendering it suitable for STD-NMR experiments (*23*), we needed to ensure that efficient magnetization transfer occurred. For large proteins, on-resonance saturation is usually set to values around −1 ppm. Because for CV-N no protein proton resonates around −1 ppm and relatively narrow lines are present, saturation frequencies were set directly on or very close to proton signals from the protein. We thus had to ascertain that the STD signal enhancements were not due to a direct saturation transfer from specific protein protons to the sugar. Therefore, several saturation frequencies were used. Investigation of the dependence of the STD-NMR spectra of the CV-N/Manα-(1→2)ManαOMe sample on the saturation frequency and saturation time (see the Supporting Information) showed that, for a saturation time of 2 s or more, similar STD spectra were obtained, indicating that full saturation of the protein by spin diffusion was achieved. A saturation time of 1 s was not sufficient for efficient transfer of saturation from the protein to the ligand protons when the saturation frequency was set at 0.25 and 7 ppm, probably because of the lower density of protein proton resonances at these frequencies and consequently insufficient saturation of all of the protein. All subsequent STD-NMR spectra were therefore recorded with the saturation frequency set at 0.4 ppm, because the methyl resonances of the protein appear in this region and irradiation at protein methyls has previously been found to yield the most effective saturation (*21*). In addition, this frequency is far away from the *O*Me signal of the sugar, such that no perturbation of this signal can be induced by the selective shaped pulse.

We also subjected samples containing ligand only (at the same concentration as used in the presence of CV-N) to STD-NMR experiments with on and off resonance frequencies set at 0.4 and 30 ppm, respectively, using saturation times of 2 and 6 s. In some cases, a small residual *O*Me signal was observed, attributable to artifacts mainly associated with

strong signals. No other signals were present in the difference spectra, indicating that the effects observed in the presence of the protein were due to true saturation transfer. In addition, we recorded control STD experiments with on and off saturation frequencies set to identical values (0.4 or 30 ppm). The resulting difference spectra were devoid of any signals, proving that good subtraction was achieved.

Last, to assess the effect of water suppression by the WATERGATE sequence, STD-NMR spectra were recorded for the CV-N/Manα(1→2)Manα*O*Me sample (2-s saturation time, off at 30 ppm and on at 0.4 ppm), with and without water suppression. No artifacts were noted using water suppression, and therefore, all STD-NMR experiments were subsequently run with WATERGATE to obtain a better S/N ratio.

RESULTS

*Interactions between Disaccharides **1**−**3** and CV-N.* We first studied the interactions between CV-N and the disaccharides, Manα(1→2)Manα*O*Me (**1**), Manα(1→3)Manα*O*Me (**2**), and Manα(1→6)Manα*O*Me (**3**) (Figure 1). These disaccharides are substructures of the oligomannoside Man-9 that is recognized by CV-N and therefore central to the antiviral properties with respect to HIV.

Among the disaccharides **1**−**3**, only **1** gave rise to large signals in the STD-NMR spectra (Figure 2a). These signals are caused by magnetization transfer from the protein to the ligand, providing direct proof of an interaction between disaccharide **1** and CV-N. Moreover, the protons of the ligand that are in closest contact with protein protons are affected more than remote protons, i.e., yield the most intense signals. All signals observed in the STD-NMR spectra for the three disaccharide complexes are listed in Table 1. In the case of disaccharide **1**, the largest STD effects were observed for H2′, H3′, and H4′ on the nonreducing end, thereby indicating that these protons have the most intimate contact with CV-N. The other protons yielded smaller STD effects, placing them at a slightly larger distance from the protein surface. Unfortunately, information about the anomeric protons could not be obtained because of the close proximity of H1 and H1′ signals to the water signal. The *O*-methyl group also yielded a strong signal at 3.35 ppm in the STD-NMR spectra. At saturation times above 0.5 s, however, its intensity in the STD-NMR spectra was smaller than that of H2′, H3′, and H4′ (see Figure 2a and the Supporting Information). Only at the shortest saturation time of 0.5 s, the *O*Me signal gave the largest STD signal. This strong signal does not reflect a close interaction of the *O*-methyl group with CV-N. It most likely is due to the fact that it is easier to observe relatively sharp signals (methyls) when the other signals are close to the level of noise (*21*).

The absence of signals in the STD-NMR spectra for the disaccharide **2** (Figure 2b) and the very weak signals in the STD-NMR spectra for **3** (Figure 2c) indicated that these two compounds did not interact significantly with CV-N.

*Interactions between Trisaccharides **4**−**7** and CV-N.* To further probe the interactions between CV-N and oligomannosides, STD-NMR experiments were performed with the linear trisaccharides Manα(1→2)Manα(1→2)Manα*O*Me (**4**), Manα(1→2)Manα(1→3)Manα*O*Me (**5**), Manα(1→2)-Manα(1→6)Manα*O*Me (**6**), and the branched trisaccharide

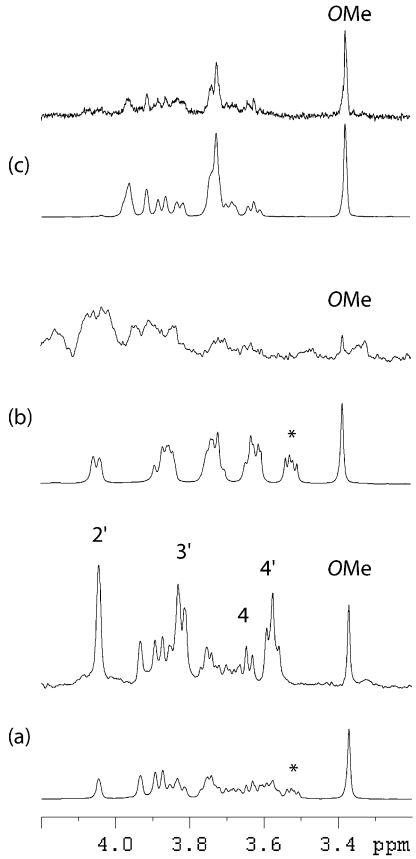

FIGURE 2: Regions of the 1D ^{1}H NMR spectra of disaccharides **1** (a), **2** (b), and **3** (c) at 600 MHz and 10 °C in the presence of CV-N. For each compound, the reference and the STD-NMR spectra, recorded with the WATERGATE sequence for water suppression, are shown. The STD-NMR spectra were recorded with on-resonance irradiation at 0.4 ppm and a saturation time of 4 s. For **2**, the broader NMR signals in the STD spectrum arise from protein resonances. The asterisks indicate a low molecular weight impurity (glycerol). Because the impurity does not bind the protein, no signals are left in the STD-NMR spectra.

Table 1: ^{1}H NMR Chemical Shifts (Parts Per Million) of the Disaccharides **1**, **2**, and **3**[a]

	H1	H2	H3	H4	H5	H6	*O*Me
1	4.994	**4.046**	**3.822**	**3.576**	3.757	3.884/3.688	
	4.991	3.934	3.846	**3.648**	3.582	3.883/3.736	3.371
2	5.090	4.044	3.854	3.632	3.722	3.859/3.741	
	4.719	4.060	3.851	3.723	3.637	3.884/3.742	3.387
3	4.884	3.964	3.825	3.625	3.685	3.873/3.731	
	4.726	3.913	3.724	3.729	3.685	3.964/3.734	3.376

[a] Resonances that exhibited strong STD effects are indicated in bold.

Manα(1→3)[Manα(1→6)]Manα*O*Me (**7**) (Figure 3). These trisaccharides mimic the branches and the core of Man-9 (Figure 1).

All trisaccharides with a terminal Manα(1→2)Manα structure exhibited signals in the STD-NMR spectra (Figure 4), providing evidence of their binding to CV-N. The largest enhancement was seen for the H2″, H3″, and H4″ protons (Figure 4 and Table 2). This observation is similar to the results obtained for the disaccharide **1**, namely, that protons in the 2, 3, and 4 position of the terminal nonreducing end residue experience the strongest effect. For trisaccharide **6**, a noticeable enhancement was also seen for H4′; this effect was less for trisaccharide **5** and absent for trisaccharide **4**.

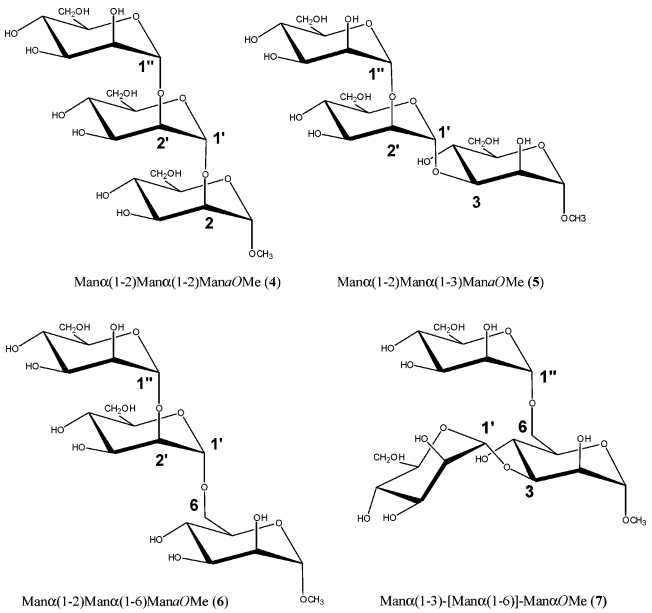

FIGURE 3: Chemical structures of trimannosides **4**−**7**.

Table 2: ^{1}H NMR Chemical Shifts (Parts Per Million) of the Trisaccharides **4**, **5**, **6**, and **7**[a]

	H1	H2	H3	H4	H5	H6	*O*Me
4	5.011	**4.042**	**3.815**	**3.590**	3.752	3.868/3.700	
	5.283	4.081	3.933	3.631	3.742	3.883/3.708	
	4.985	3.909	3.840	3.651	3.587	3.883/3.741	3.370
5	5.011	**4.041**	**3.822**	**3.625**	3.712	3.820/3.724	
	5.333	4.068	3.964	**3.678**	3.727	3.854/3.740	
	4.707	4.043	3.825	3.718	3.621	3.876/3.728	3.376
6	5.002	**4.049**	**3.827**	**3.587**	3.770	3.876/3.697	
	5.142	3.989	3.939	**3.670**	3.727	3.873/3.742	
	4.725	3.914	3.726	3.726	3.675	3.950/3.724	3.377
7	5.071	4.039	3.859	3.636	3.740	3.856/3.735	
	4.881	3.974	3.818	3.639	3.661	3.876/3.735	
	4.700	4.072	3.839	3.889	3.794	4.013/3.688	3.384

[a] Resonances that exhibited strong STD effects are indicated in bold.

Figure 2a and parts b and c of Figure 4 clearly show that the STD-NMR spectra for trisaccharides **5** and **6** are very similar to the STD-NMR spectrum for disaccharide **1**, exhibiting strong signals for H2, H3, and H4 of the terminal unit and a clear but smaller enhancement for H4 of the penultimate unit. In contrast, the STD-NMR spectrum (Figure 4a) for the linear trisaccharide **4** differed, because only slight enhancements of the H2″, H3″, and H4″ signals of the terminal mannose residue were observed. This indicates that trisaccharide **4** effectively binds to CV-N, albeit in a different fashion compared to oligomannosides **1**, **5**, and **6**. It is also worth pointing out that for identical concentrations the STD signal intensities obtained for trisaccharide **4** were lower than those obtained for **1**, **5**, and **6**. Because for k_d values in the milli- to micromolar range, the STD-NMR effects are independent of the off rate (*24*), the smaller STD intensities observed for **4** might reflect either a higher binding affinity or binding to a different site.

The branched trisaccharide **7** (Figure 4d) yielded no signals in the STD experiment, demonstrating that this compound did not interact to any appreciable degree with CV-N.

DISCUSSION

Using STD-NMR, we were able to define the minimum oligomannoside structure required for high-affinity binding

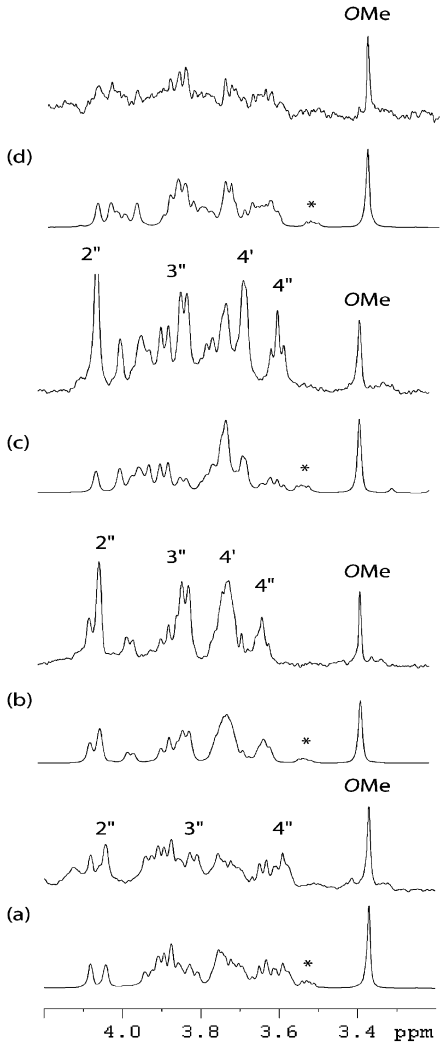

FIGURE 4: Regions of the 1D ^{1}H NMR spectra of trisaccharides **4**−**7** (a−d) at 600 MHz and 10 °C in the presence of CV-N. For each compound, the reference and the STD-NMR spectra, recorded with the WATERGATE sequence for water suppression, are shown. The STD-NMR spectra were recorded with on-resonance irradiation at 0.4 ppm and a saturation time of 4 s. The asterisks indicate a low molecular weight impurity (glycerol). Because the impurity does not bind the protein, no signals are left in the STD-NMR spectra.

to CV-N. Our present results are in good agreement with previous crystallographic and NMR titration studies that implicated a terminal disaccharide Manα(1→2)Manα unit as essential for the binding affinity. We confirmed the importance of the α(1→2) linkage notably by demonstrating that the disaccharides **2** and **3** as well as the trisaccharide **7** did not yield STD-NMR signals, whereas **1** and the linear trisaccharides **4**, **5**, and **6** clearly displayed saturation transfer from the protein to the 2, 3, and 4 protons of the terminal nonreducing sugar unit. The absence of STD signals for the core trimannoside (**7**), another substructure of Man-9, also substantiates previous NMR and calorimetric studies (*15*) that showed that **7** did not bind to CV-N.

The interaction between CV-N and oligomannosides is mainly driven by the terminal residue, as evidenced by the largest enhancements in all of the STD-NMR spectra. Only the α(1→2) linkage allows the sugars to take a conformation in which the nonreducing mannopyranose ring can stack over the penultimate mannopyranose ring. Such a conformation

is not favorable with a (1→3) or (1→6) linkage. The stacked conformation results in a compact structure that is able to penetrate into the binding sites of CV-N. STD-NMR spectroscopy also allowed defining the binding epitope on the sugar at the atomic level. The H2, H3, and H4 positions of the terminal nonreducing mannose in **1**, **5**, and **6** experience more saturation transfer from the protein than any other protons and therefore have to be in closest contact with the protein. In addition, the H4 resonance of the penultimate sugar unit also experienced enhancement. The similarities observed in the STD-NMR spectra for the above three compounds suggest a similar binding interaction with CV-N. In contrast, the STD-NMR spectrum of **4** was markedly different and displayed more homogeneous enhancements for all resonances, albeit with smaller STD intensities. These smaller STD signals reflect either tighter binding or a different mode of interaction for **4** compared to **1**, **5**, and **6**. If binding is very tight (in the nanomolar range), then saturation transfer to ligand molecules is not very efficient and small STD effects are generally observed, whereas for weak association, fast exchange between the free and bound ligand leads to a very efficient build up of saturation of the ligand molecules in solution and large STD effects are observed. However, when binding becomes very week (>10 mM), the probability of the ligand being in the receptor site becomes very low, which results in weak STD signals. In principle, the presence of small STD signals for **4** could be caused by much tighter or weaker binding compared to compounds **1**, **5**, and **6**, but given the fact that all four sugars bind to CV-N with affinity constants in the 10^{-4} to 10^{-6} M range (*12*, *14*), the smaller intensities in the STD-NMR spectra for **4** are most likely caused by a different binding mode.

A previous study showed that **1**, **5**, and **6** bind to CV-N at both binding sites with comparable affinity, while the trisaccharide **4** exhibits a slight preference for one of the sites**.** Our STD-NMR spectra correlate well with these results. The recognition site on domain B of CV-N consists of a deep pocket, and the H2, H3, and H4 protons of the nonreducing end of the disaccharide **1** are in close contacts with the protein (*13*) (Figure 5b). For the sugar-binding site on domain A (residues 1−38/90−101), which displays a more open structure, the distances between the terminal H2, H3, and H4 protons and the surface of the protein are larger (>4 Å) (Figure 5a). It is interesting that the STD results clearly revealed the ability of CV-N to discriminate between three structurally related trisaccharides. This indicates that not only the terminal disaccharide but also the reducing mannose residue influences the affinity and the selectivity in the interaction with CV-N. Most likely, the conformation of the glycosidic linkage between the common terminal disaccharide and the reducing mannopyranose ring is responsible for the observed selectivity.

Further studies will involve the interaction between CV-N and (1→2)-linked disaccharides where the mannopyranoside has been replaced by sugars having different configurations of their hydroxy groups. These studies should reveal whether the precise location of the hydroxyl groups is a crucial determinant for binding. In addition, the study of CV-N mutants, with only one binding site, in combination with STD-NMR spectroscopy should permit defining the molecular epitopes involved in the interaction at each individual binding site. Furthermore, because the antiviral activity of CV-N is a consequence of its binding to carbohydrates, understanding the structural basis of such an interaction would allow for the development of new molecules able to compete with HIV receptors present on cell surfaces.

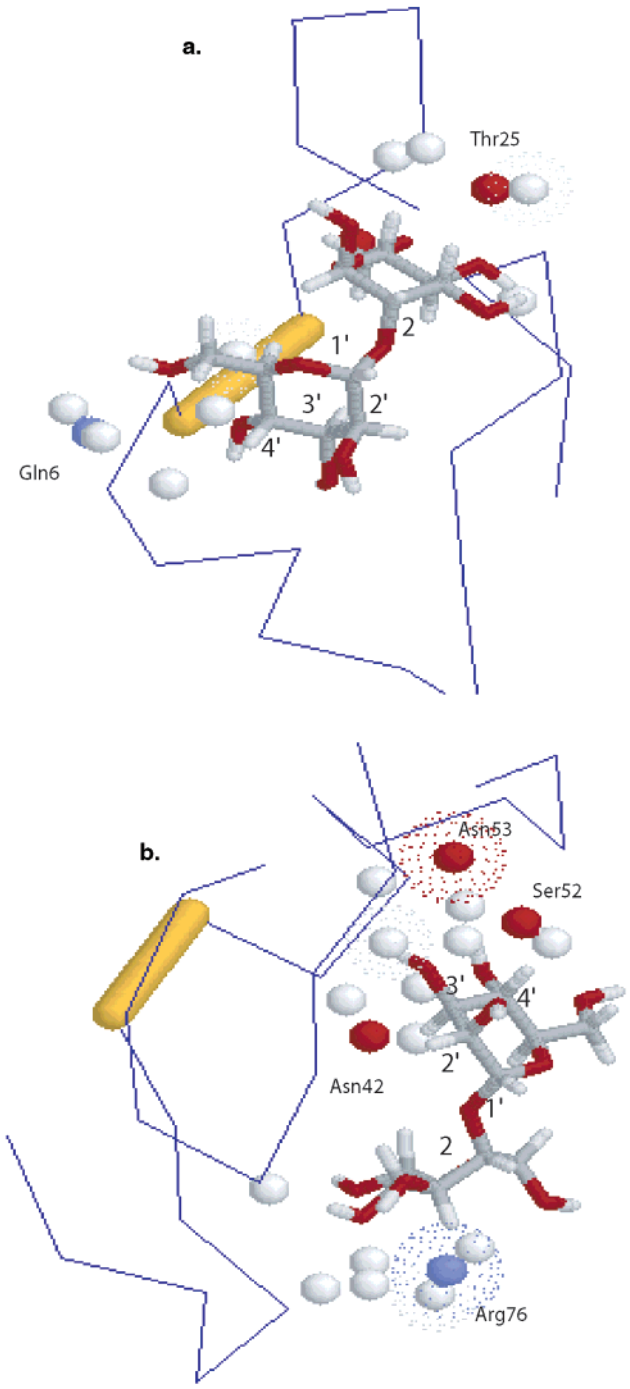

FIGURE 5: Conformation of the disaccharide Manα(1→2)Manα as modeled into the two carbohydrate-binding sites on CV-N (taken from ref 13, PDB code 1iiy). (a) Manα(1→2)Manα bound to the site on domain A (residues 1−38/90−101), and (b) Manα(1→2)-Manα bound to the site on domain B (residues 39−89). The backbone structure of CV-N is shown in blue lines; the disulfide bond is shown as a yellow rod; and selected atoms of those amino acids of CV-N that line the binding pockets are shown as white (H), red (O), or blue (N) spheres. Their identity is given by the amino acid name and number. The figure was generated with MDL Chime.

SUPPORTING INFORMATION AVAILABLE

1D STD-NMR spectra of Manα(1→2)Manα*O*Me, Manα-(1→2)Manα(1→2)Manα*O*Me, Manα(1→2)Manα(1→3)-Manα*O*Me, and Manα(1→2)Manα(1→6)Manα*O*Me in the presence of CV-N at 10 and 25 °C. 1D STD-NMR spectra of Manα(1→2)Manα*O*Me in the presence of CV-N obtained with varying saturation frequencies and saturation times. This material is available free of charge via the Internet at http://pubs.acs.org.

REFERENCES

1. Boyd, M. R., Gustafson, K. R., McMahon, J. B., Shoemaker, R. H., O'Keefe, B. R., Mori, T., Gulakowski, R. J., Wu, L., Rivera, Laurencot, C. M., Currens, M. J., Cardellina, J. H., II, Buckheit, R. W., Jr., Nara, P. L., Pannell, L. K., Sowder, R. C., II, and Henderson, L. E. (1997) Discovery of cyanovirin-N, a novel human immunodeficiency virus-inactivating protein that binds viral surface envelope glycoprotein gp120: Potential applications to microbicide development, *Antimicrob. Agents Chemother. 41*, 1521−1530.
2. Dey, B., Lerner, D. L., Lusso, P., Boyd, M. R., Elder, J. H., and Berger, E. A. (2000) Multiple antiviral activities of cyanovirin-N: Blocking of human immunodeficiency virus type 1 gp120 interaction with CD4 and coreceptor and inhibition of diverse enveloped viruses, *J. Virol. 74*, 4562−4569.
3. Barrientos, L. G., O'Keefe, B. R., Bray, M., Sanchez, A., Gronenborn, A. M., and Boyd, M. R. (2003) Cyanovirin-N binds to the viral surface glycoprotein, GP1,2 and inhibits infectivity of Ebola virus, *Antiviral Res.*, *58*, 47−56.
4. Esser, M. T., Mori, T., Mondor, I., Sattentau, Q. J., Dey, B., Berger, E. A., et al. (1999) Cyanovirin-N binds to gp120 to interfere with CD4-dependent human immunodeficiency virus type 1 virion binding, fusion, and infectivity but does not affect the CD4 binding site on gp120 or soluble CD4-induced conformational changes in gp120, *J. Virol. 73*, 4360−4371.
5. O'Keefe, B. R., Shenoy, S. R., Xie, D., Zhang, W., Muschik, J. M., Currens, M. J., Chaiken, I., and Boyd, M. R. (2000) Analysis of the interaction between the HIV-inactivating protein cyanovirin-N and soluble forms of the envelope glycoproteins gp120 and gp41, *Mol. Pharmacol. 58*, 982−992.
6. Bolmstedt, A. J., O'Keefe, B. R., Shenoy, S. R., McMahon, J. B., and Boyd, M. R. (2001) Cyanovirin-N defines a new class of antiviral agent targeting N-linked, high mannose glycans in an oligosaccharide-specific manner, *Mol. Pharmacol. 59*, 949−954.
7. Shenoy, S. R., O'Keefe, B. R., Bolmstedt, A. J., Cartner, L. K., and Boyd, M. R. (2001) Selective interactions of the human immunodeficiency virus-inactivating protein cyanovirin-N with high-mannose oligosaccharides on gp120 and other glycoproteins, *J. Pharmacol. Exp. Ther. 297*, 704−710.
8. Bewley, C. A., Gustafson, K. R., Boyd, M. R., Covell, D. G., Bax, A., Clore, G. M., and Gronenborn, A. M. (1998) Solution structure of cyanovirin-N, a potent HIV-inactivating protein, *Nat. Struct. Biol. 5*, 571−578.
9. Yang, F., Bewley, C. A., Louis, J. M., Gustafson, K. R., Boyd, M. R., Gronenborn, A. M., et al. (1999) Crystal structure of cyanovirin-N, a potent HIV-inactivating protein, shows unexpected domain swapping, *J. Mol. Biol. 288*, 403−412.
10. Barrientos, L. G., Louis, J. M., Botos, I., Mori, T., Han, Z., O'Keefe, B. R., Boyd, M. R., and Gronenborn, A. M. (2002) The domain-swapped dimer of cyanovirin-N is in a metastable folded state. Reconciliation of X-ray and NMR structures, *Structure 10*, 673−686.
11. Botos, I., O'Keefes, B. R., Shenoy, S. R., Cartner, L. K., Ratner, D. M., Seeberger, P. H., Boyd, M. R., and Wlodawer, A. (2002) Structures of the complexes of a potent anti-HIV protein cyanovirin-N and high mannose oligosaccharides, *J. Biol. Chem. 277*, 34336−34342.
12. Bewley, C. A., and Otero-Quintero, S. (2001) The potent anti-HIV protein cyanovirin-N contains two novel carbohydrate binding sites that selectively bind to Man(8) D1D3 and Man(9) with nanomolar affinity: Implications for binding to the HIV envelope protein gp120, *J. Am. Chem. Soc. 123*, 3892−3902.
13. Bewley, C. A. (2001) Solution structure of a cyanovirin-N: Manα1−2Manα complex: Structural basis for high-affinity carbohydrate-mediated binding to gp120, *Structure 9*, 931−940.
14. Bewley, C. A., Kiyonaka, S., and Hamachi, I. (2002) Site-specific discrimination by cyanovirin-N for a-linked trisaccharides comprising the three arms of Man_8 and Man_9, *J. Mol. Biol. 322*, 881−889.
15. Shenoy, S. R., Barrientos, L. G., Ratner, D. M., O'Keefe, B. R., Seeberger, P. H., Gronenborn, A. M., and Boyd, M. R. (2002) Multisite and multivalent binding between cyanovirin-N and branched oligomannosides: Calorimetric and NMR characterization, *Chem. Biol. 9*, 1109−1118.
16. Chang, L. C., and Bewley, C. A. (2002) Potent inhibition of HIV-1 fusion by cyanovirin-N requires only a single high affinity carbohydrate binding site: Characterization of low-affinity carbohydrate binding site knockout mutants, *J. Mol. Biol. 318*, 1−8.
17. Barrientos, L. G., Louis, J. M., Ratner, D. M., Seeberger, P. H., and Gronenborn, A. M. (2003) Solution structure of a circular-permuted variant of the potent HIV-inactivating protein cyanovirin-N: Structural basis for protein stability and oligosaccharide interaction, *J. Mol. Biol. 325*, 211−223.
18. Mayer, M., and Meyer, B. (1999) Characterization of ligand binding by saturation transfer difference NMR spectroscopy, *Angew. Chem., Int. Ed. 38*, 1784−1788.
19. Mayer, M., and Meyer, B. (2001) Group epitope mapping by saturation transfer difference NMR to identify segments of a ligand in direct contact with a protein receptor, *J. Am. Chem. Soc. 123*, 6108−6117.
20. Klein, J., Meinecke, R., Mayer, M., and Meyer, B. (1999) Detecting binding affinity to immobilized receptor proteins in compound libraries by HR-MAS STD NMR, *J. Am. Chem. Soc. 121*, 5336−5337.
21. Yan, J., Kline, A. D., Mo, H., Shapiro, M. J., and Zartler, E. R. (2003) The effect of relaxation on the epitope mapping by saturation transfer difference NMR, *J. Magn. Reson. 163*, 270−276.
22. Piotto, M., Saudek, V., and Sklenar, V. (1992) Gradient-tailored excitation for single-quantum NMR spectroscopy of aqueous solutions, *J. Biomol. NMR 2*, 661−665.
23. Meyer, B., and Peters, T. (2003) NMR spectroscopy techniques for screening and identifying ligand binding to protein receptors, *Angew. Chem., Int. Ed. 42*, 864−890.
24. Jayalakshmi, V., and Krishna, N. R. (2002) Complete relaxation and conformational exchange matrix (CORCEMA) analysis of intermolecular saturation transfer effects in reversibly forming ligand−receptor complexes, *J. Magn. Reson. 155*, 106−119.

BI048676K